ACS OMEGA

http://pubs.acs.org/journal/acsodf

Mini-Review

Influence of Nanofillers on Adhesion Properties of Polymeric Composites

Aparna Guchait, Anubhav Saxena, Santanu Chattopadhyay,* and Titash Mondal*

Cite This: *ACS Omega* 2022, 7, 3844−3859

Read Online

ACCESS | Metrics & More | Article Recommendations

ABSTRACT: Nanofillers (NFs) are becoming a ubiquitous choice for applications in different technological innovations in various fields, from biomedical devices to automotive product portfolios. Potential physical attributes like large surface areas, high surface energy, and lower structural imperfections make NFs a popular filler over microfillers. One specific application, where NFs are finding applications, is in adhesive science and technology. Incorporating NFs in the adhesive matrix is seen to tune the adhesives' different properties like wettability, rheology, etc. Additionally, the functional benefits (like electrical/thermal conductivity) of these NFs are translated into the adhesives' properties. Such an improvement in the properties is far to achieve using microfillers in the adhesive matrix. This mini-review provides an account of the impact of the addition of various nanofillers (NFs) on the properties of the adhesive composition.

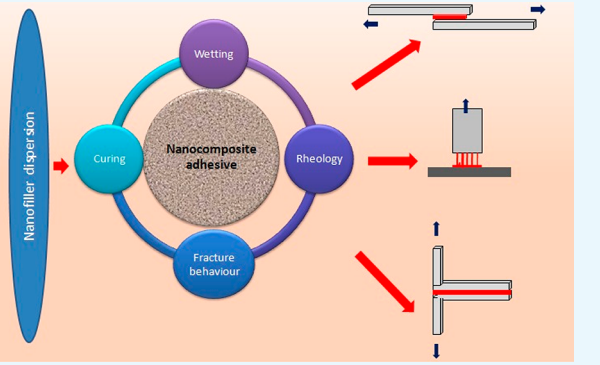

1. INTRODUCTION

In the last few decades, there has been widespread research related to adhesive science and technology in various domains such as automotive, aerospace, construction, defense, marine, electronics, and other industries. The adhesive is the substance capable of binding similar or dissimilar materials together, such as metals, ceramics, polymers, and composites, by intimate surface contact via interfacial forces. These interfacial forces may arise from chemical bonding, electrostatic attraction, and secondary interactions such as van der Waals, hydrogen bonding, etc.[1a] The performance of the adhesive can be influenced by the physicochemical properties of the adhesive and adherend, nature of the surface preparation and pretreatment, wetting of the surface, joint design, and adhesion process (curing).[1b] The mechanical properties are influenced by the formulation of the adhesive, joint design of the structure, and the applied load distribution mechanism throughout the adhesive and adherend. Adhesives can be classified into multiple segments. The classification mainly relies on the following parameters, based on their (i) curing mechanism (functional groups it leverages to cross-link), (ii) form factor (e.g., dispensable, coatable, sprayable, meltable, etc.), (iii) their application type (e.g., application of adhesive by application of pressure, heat, etc.), and (iv) load-bearing nature (higher or lower than 1000 psi).[1c] It is worth mentioning that the concept of adhesion is utilized in various segments, including paints and coating, etc. The macroscopic evaluation of the properties of a polymer composite can also be explained in terms of adhesion forces acting between filler and the polymer. Hence, it can be unequivocally suggested that there is a pressing need to understand the physics and chemistry governing the different fields of materials innovation.

The overall bonding effectiveness of the adhesive is determined by the combination of cohesive and adhesive strengths. The cohesive strength is defined as the intramolecular attraction between the similar materials due to various interactions between the adhesive molecules, whereas adhesive strength is the same for dissimilar materials (i.e., adhesive and substrate). A strong and stable adhesive bond formation requires the establishment of interfacial molecular interaction, wherein interface refers to the interacting sites. Various mechanisms can explain intrinsic adhesive forces across the interface.[1d] These mechanisms include mechanical interlocking, electrostatic, diffusion, chemical bonding, adsorption or wetting, and boundary layer theory.[1d] The adhesive should wet and spread over the adherend surface for strong adhesive interaction. Insufficient wetting can lead to bubble entrapment and lesser contact with the material, resulting in poor adhesive strength.[2a] Despite multiple ways that are possible to augment the performance attributes of an adhesive

Received: September 30, 2021
Accepted: January 12, 2022
Published: January 25, 2022

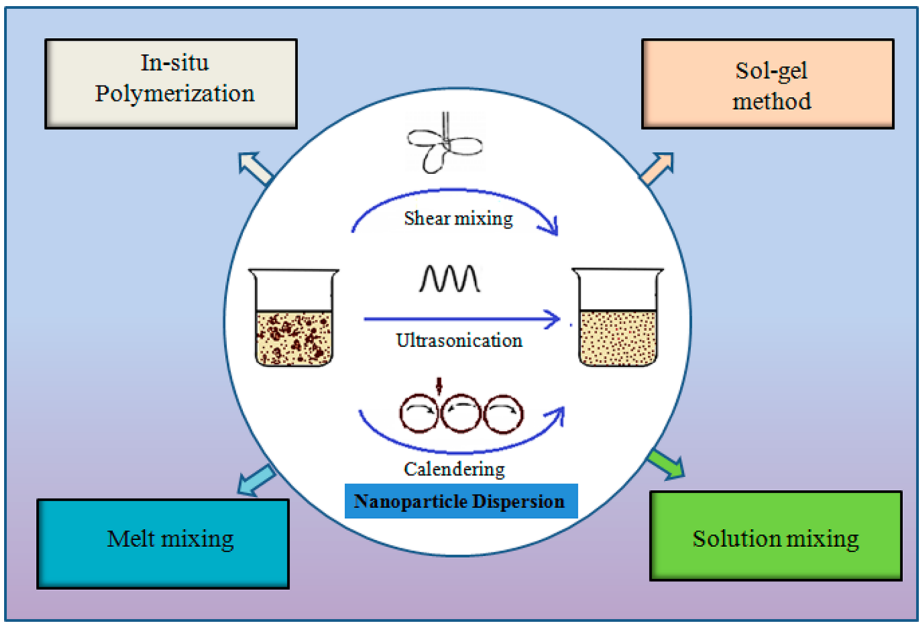

Figure 1. Different techniques to fabricate nanocomposite-adhesive systems.

performance, the addition of filler into the system is the easiest and most popular.

Myriads of research works have been explored to study the impact of the incorporation of nanofillers into polymers. Typically, such polymer-nanocomposites exhibit much higher mechanical, thermal, and other multifunctional properties than conventional polymer composites prepared with microfillers. The unique interface created between the polymer and the nanofiller demonstrates improved performances of such composites. Owing to the large specific surface area of the nanofillers, the number of filler−polymer matrix interaction sites (interfaces) increases in the well dispersed polymer nanocomposites. These interfaces plays a critical role toward controlling the properties of the nanocomposites. Similar observations are made in the adhesive composition prepared with nanofillers. Adhesive properties like the coefficient of wetting, interfacial free energy, and work of adhesion are mainly impacted by the nanofillers' presence. The incorporation of various nanofillers into the adhesive system has been reported in the literature in recent years. Fillers of different shapes and sizes have been explored for the development of the composite, with nanosilica, nanoalumina, different varieties of carbonaceous nanofillers, and layered silicates being the most commonly used nanofillers.[2b]

Such nanocomposite adhesive improves the mechanical, rheological, thermal, and fire resistance properties. Specific properties such as moisture, gas permeability, and electrical conductivity, etc. are also impacted.[2c−e] However, it is worth mentioning that incorporating nanofillers in the adhesive to achieve illustrious properties is challenging. The said caveat is attributed to the challenges involved in dispersing the nanofiller in the matrix. Uniform filler dispersion in the adhesive matrix is required to achieve improved properties of the nanofilled adhesive system. For instance, the dispersion of layered silicates in the polymer matrix happens mostly via phase-separation, intercalation, or exfoliation mechanisms. The properties of phase segregated layer silicate nanocomposite compositions are inferior to the exfoliated or the intercalated derivatives. Other factors like filler loading, size, orientation, and aspect ratio in the adhesive composition remarkably affect the properties.[3a,b] Maximum adhesion strength is achieved at an optimum filler loading. For instance, adding 1.5 wt % nanoalumina in adhesive composition can increase the lap shear strength and tensile strength by ∼40% and ∼60%, respectively.[4] The filler concentration beyond the said window negatively impacts the properties. Hitherto, it can be unequivocally suggested that the addition of the nanofillers significantly impacts the functional attributes of the polymer nanocomposite adhesives; however, a comprehensive review on discussing the critical parameter controlling the properties/performance of the polymer nanocomposite adhesive is far and few. This mini-review will discuss such critical factors that influence the adhesion properties and performance of polymer nanocomposite adhesives.

2. DISPERSION OF NANOFILLER IN THE ADHESIVE SYSTEM

Nanofillers (NFs) are ultrafine particles with at least one size aspect in the nanorange (1−100 nm). A variety of NFs like carbon nanotubes, graphene, nanoclays, etc. have been introduced to various adhesive matrixes to improve overall joint strength.[5a] Anisotropic layered fillers like nanographite, graphene, nanoclays, or the tubular shaped filler like carbon nanotubes (multiwalled and single walled) are among the favorite filler materials used in the formulation. It is worth mentioning that isotropic particles like nanosilica are also equally investigated in the adhesive formulation. The final properties of the composite adhesive depend on the uniform distribution of nanofiller into the system. A challenging fact is involved in dispersing the nanomaterials in the matrix. The higher surface area of the nanomaterials leads to the formation of a large-scale agglomerate in the matrix. However, this dispersion process is tricky as the filler loading is increased in the matrix. The polymer system's viscosity increases with the volume fraction of NFs. For instance, CNTs tend to self-assemble in bundlelike structures along their length axis, acting as stress concentrations within the polymer nanocomposite, thus leading to property deterioration. Graphenes are single-

https://doi.org/10.1021/acsomega.1c05448
ACS Omega 2022, 7, 3844−3859

layer sheets composed of two-dimensional carbon arranged in a honeycomb structure. Multiple layers of graphene sheets stack together by van der Waals forces. This stacking nature of graphene sheets restricts efficient polymer interaction.[5b]

In the same way, nanoclays form platelet structures by stacking clay layers, making it difficult for polymer chains to penetrate between the clay layers. The properties of nanoplatelet-based composites can only be enhanced by the diffusion of the polymer chains into the interlayer of the layered nanoparticles (i.e., intercalated or exfoliated). It should also be noted that if the size of the nanofiller agglomeration is equivalent to the size of the usual surface pores, this may restrict the adhesive to fill in the pore. As a result, lower agglomeration should result in greater contact with the substrate and, as a result, improved adhesion strength.

Different methodologies are adopted to prepare nanocomposite adhesives. Guided by the type of nanofillers, polymer matrix, and applications, techniques such as in situ polymerization, the sol−gel method, melt mixing, and solution mixing are adopted (Figure 1).[5c] Mechanical stirring is used in every technique to disperse NFs in the polymer, which includes several methods like shear mixing, calendaring, and ultrasonic mixing. Ultrasonic irradiation exploits sound waves to disperse particles in the continuous phase (frequency >20 kHz). Ultrasonication produces high-pressure liquid waves, which lead to the formation and collapse of microbubbles. This process is also termed ultrasonic cavitation that develops high-speed liquid jets. These hydrodynamic shear forces create strong pressure on the particle agglomerate to separate the particles from each other. However, it is worth mentioning that the NFs can be seriously damaged if sonication is done for a longer time. Calendering is known to be a high shear process, wherein the composite is made to pass through three rollers. This squeezing of the composite in between the rolls results in improved dispersion. The gap distance and the number of cycles significantly impact the dispersion in the calendaring process. A rotating blade capable of producing a high shear rate can also be leveraged to prepare the nanocomposite. A vortex is created due to the blade's presence, which helps in the dispersion of the filler in the matrix.

Techniques involving mixing the nanoparticle in the solution state with the polymer matrix yield a good dispersion of the filler. Similarly, polymerization in the presence of nanoparticles also improves the dispersion.[5d] The solution mixing technique involves the dispersion of nanofiller in a solvent often by leveraging ultrasonication followed by the evaporation of the solvent to get the composite. In-situ polymerization technique, nanofillers are swollen in the monomer solution, and then polymerization is carried out. As a result, an exfoliated or intercalated superstructure is formed. This technique is particularly suitable for insoluble or thermal unstable polymers as they cannot be dissolved in solvents or fused. The melt mixing process involves the melting of the polymer followed by the addition of the nanofillers in the melt to develop the composite. The dispersion is achieved with the aid of a high shear rate. Another popular technique of NF dispersion is the sol−gel method. Sol refers to a colloidal dispersion of solid nanoparticles. Typically in the gel phase, the networks are interconnected with each other in the three-dimensional space. The nanoparticle solution in monomer acts as the sol phase, whereas the polymerization of the monomers present in the sol phase attributes toward the gel phase. The polymer acts as a nucleating agent, allowing stacked crystals to develop. The polymer seeps between layers as the crystals grow, forming a nanocomposite. The sol−gel processing technology enables the development of high purity material with a uniform dispersion of NFs in the matrix.

The continuous interface among the nanofiller and matrix can be established by modifying the surface of NFs, which significantly reduces filler agglomeration and improves dispersion and compatibility of NFs within the polymer matrix, thus enhancing the properties of the nanocomposite.[5e]

Myriads of functional groups ranging from alcohol to epoxy can be leveraged to tune the surface of the nanofiller. Apart from introducing only the functional groups, grafting suitable polymeric side chains onto the NFs can meet the purpose well. The strong interfacial adhesion between the modified NFs and polymeric matrix can be explained by cocrystallization, chain entanglement, and secondary interactions such as hydrogen bonding.[6a−c] Various methods have been developed for surface modification of nanomaterials that produce superior hybrid nanocomposites with improved properties.

3. INFLUENCE OF NFS ON STRUCTURAL FACTORS CONTRIBUTING ADHESION PROPERTIES

The performance of an adhesive bond is characterized by interfacial adhesive strength and cohesive strength. Typically, the failure mode can be classified as (i) adhesive and (ii) cohesive type. During the debonding phase, weak interfacial strength leads to adhesive failure, and thereby, the adhesive fails from the interface. In contrast, the failure of the adhesive from the bulk is referred to as the cohesive mode of failure. Depending on various parameters, the adhesive can fail in either of the ways.

3.1. Wettability. A critical factor for the strong interfacial adhesion strength is the excellent wetting behavior of the adhesive, which allows the adhesive to cover the substrate surface. Insufficient wetting of the substrate by the adhesive causes bubble entrapment at the joint. This further leads to reduced adhesion strength or adhesive failure. For efficient wetting, surface energetic plays a critical role and is governed by Young's equation (three-phase contact as shown in Figure 2). Typically, as a rule of thumb, surface energy of the substrate should be higher than that of the adhesives. The Young's equation is given by

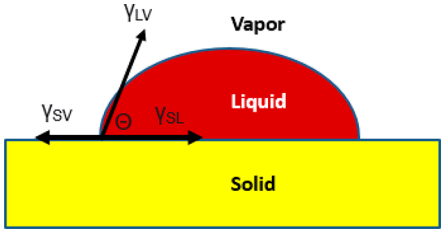

Figure 2. Young's equation demonstration of the three-phase line.

$$\gamma_{SV} = \gamma_{SL} + \gamma_{LV} \cos\theta \quad (1)$$

where γ_{SV}, γ_{SL}, γ_{LV}, and θ represent the surface tensions between the solid (S)-vapor (V), solid (S)-liquid (L), and liquid (L)-vapor (V) interfaces and contact angle, respectively. For effective wetting of the substrate, θ should be zero. Hence, effective wetting can be represented with P_s as the spreading constant

https://doi.org/10.1021/acsomega.1c05448
ACS Omega 2022, 7, 3844−3859

$$\gamma_{SV} \geq \gamma_{SL} + \gamma_{LV} \quad (2)$$

$$P_s = \gamma_{SV} - \gamma_{SL} - \gamma_{LV} \quad (3)$$

According to Dupre's equation, the work of adhesion in creating a new surface between a solid and liquid surface during the wetting process can be expressed by the following equation,

$$W_{SL} = \gamma_{SV} + \gamma_{LV} - \gamma_{SL} \quad (4)$$

By considering Young's equation, the above equation can be written as

$$W_{SL} = \gamma_{LV}(1 + \cos\theta) \quad (5)$$

The higher work of adhesion implies stronger bonding. Considering Fowkes' theory, the surface energy can be calculated by the combination of the dispersive component (D) and the nondispersive or polar component (P), which is given by

$$\gamma = \gamma^D + \gamma^P \quad (6)$$

The work of adhesion can be expressed by

$$W_{SL} = W^D + W^P = 2\left(\sqrt{\gamma_S^D \cdot \gamma_L^D} + \sqrt{\gamma_S^P \cdot \gamma_L^P}\right) \quad (7)$$

Khalil et al.[7a] showed the influence of the alumina nanoparticle (ANF) incorporation on the wetting property of the nanofilled epoxy adhesive prepared by the solution technique. The addition of ANF impacted the contact angle. As a result, the wettability of the adhesive was improved (Figure 2). The contact angle of nonreinforced epoxy adhesive was decreased with the increment of the ANF concentration, indicating the better wettability of the nanofilled adhesive. This improved wettability was explained by the more considerable difference in surface and interface free energy for nanoparticles. This was attributed to then a nanoparticle's higher surface free energy. A hydrophilic character was induced in the adhesive, thus increasing the wettability. In another study, the influence of zirconia nanoparticle addition on the wetting behavior of the epoxy adhesive was conducted.[7b] The contact angle of water on pure epoxy, nanofilled adhesive, and the aluminum adherent was evaluated. The measured equilibrium contact angle for pure epoxy was 82.1°, for epoxy−zirconia (0.5 vol %) composite adhesive was 71.5°, while for the aluminum substrate, it was 59.4°. The result indicated a significant decrease in the equilibrium contact due to the incorporation of zirconia. Moreover, the contact angle was slightly increased with the higher zirconia concentration. This observation can be explained by the fact that a higher nanofiller concentration leads to a poor degree of dispersion due to the formation of agglomerates.[7b] A similar effect was observed when the water contact angle was measured for nanoparticle-filled acrylic adhesive application on steel substrates.[7c] The result showed a reduced equilibrium contact angle from 138.1° for the pure acrylic adhesive. The values for the nanocomposites changed to 93.9°, 100.1°, and 92.2°, with a filler loading of 1.5 wt % nano-Al_2O_3, nano-SiO_2, and nano-TiO_2, respectively. This clearly indicated a significant decrease in contact angle due to the incorporation of nanoparticles, as shown in Figure 3.[7c] Therefore, it can be concluded that the inclusion of NFs in the adhesive formulation resulted in slightly improved wettability at the interfaces and greater compatibility between the adhesive and the substrate. This results in a higher adhesive strength for the developed material.

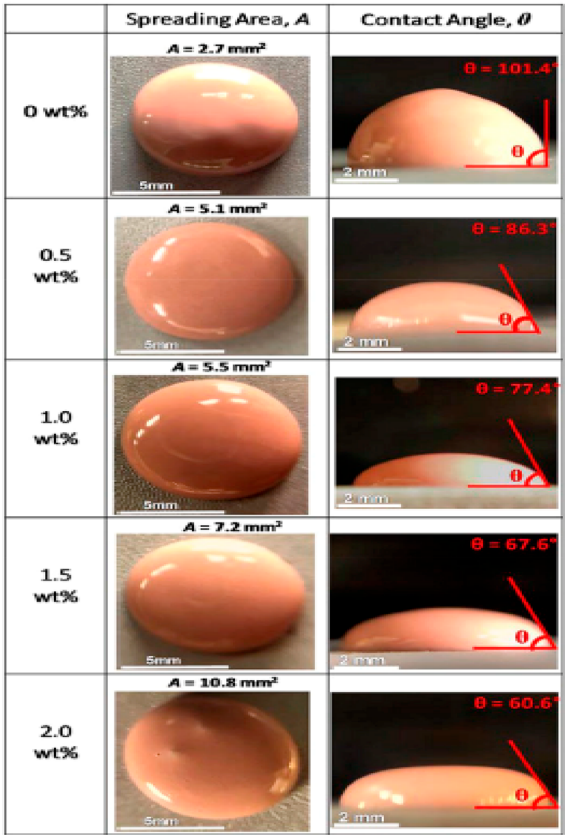

Figure 3. Optical image of the spreading area and contact angle measurement of ANF filled adhesive on aluminum substrate. Reprinted with permission from ref 7a. Copyright 2019 Elsevier.

3.2. Rheology. Rheology of an adhesive is an important characteristic to study the flow or deformation behavior of the adhesive. Viscosity and viscoelasticity are the most significant measure of the same. The viscosity of the nanocomposite adhesive increases with the addition of NFs. As a result, a slow wetting of the nanofilled adhesive to the adherend is observed. It is worth mentioning, depending on the type of nanofillers, the viscosity might decrease as well.[8a] The higher viscosity may be advantageous, as it aids in preventing adhesive leaking from the gap between the substrates. On the contrary, a drop in viscosity is beneficial for good wetting. An increase in the viscosity results from uniform dispersion of NFs (exfoliated or intercalated) without agglomeration. In the case of stratified shear flow occurring in the low viscous regime inside the thin layer of the dispersion media, a shifting of the sample is observed in the direction of flow. As a result, the assembly within this block remains unchanged. Furthermore, the flow of the anisotropic particles under rotational forces exacerbated the problem further by developing a series of regular matrix−filler layers.[8b]

For example, the rheological attributes of epoxy-montmorillonite (MMT) nanocomposites at a filler loading of 2 and 5% were investigated by Ilyin et al.[8c] The rheological data indicated that the ultrasonication improved the dispersion of organomodified MMT in the epoxy resin, resulting in increased viscosity. Enhanced agglomerate formation and, consequently, the appearance of the yield stress in the case of the unmodified MMT Cloisite Na^+ resulted in reduced

https://doi.org/10.1021/acsomega.1c05448
ACS Omega 2022, 7, 3844−3859

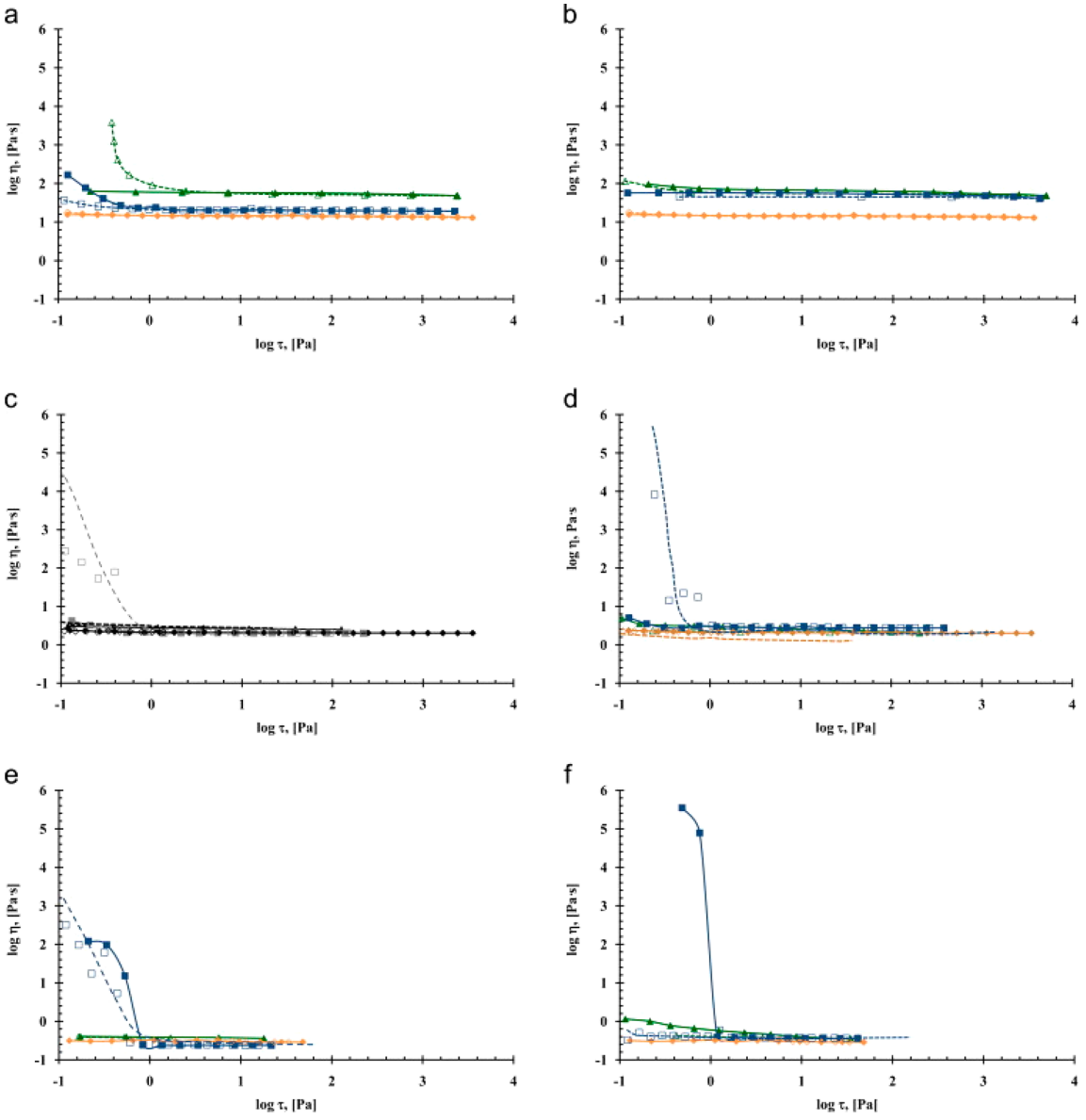

Figure 4. Graphical representation on viscosity of Cloisite Na^+ filled composite adhesive at 2 wt % (a, c, e) and 5 wt % (b, d, f) loading and at 20 °C (a, b), 40 °C (c, d), and 60 °C (e, f). Green ▲ and blue ■ represents 0 and 4 min ultrasonication time, respectively. A gold ◆ indicates unfilled adhesive. Reprinted with permission from ref 8c. Copyright 2015 Elsevier.

viscosity. The viscosity dependence of nanocomposite adhesive with different NF concentrations at various temperatures is shown in Figure 4 and Figure 5. A high degree of incompatibility between the hydrophilic layered silicates and the hydrophobic polymers is noted. It can be improved via surface modification of such hydrophilic materials with different organic components. Thus, the addition of organo-modified Cloiste 30B into the epoxy resin resulted in uniform dispersion due to the formation of hydrogen bonds between 2-hydroxyethyl groups of the Cloisite 30B and the polar ends of the epoxy oligomer. Thus, the surface nature significantly influences the rheology.[8c] A similar result could also be observed for non-cross-linked polyisobutylene (PIB)-based pressure-sensitive adhesive (PSA) filled with natural, un-modified Cloisite Na^+ and organomodified Cloisite 15A clay. PIB-Cloisite 15A composite demonstrated higher viscosity than natural Cloisite Na^+ containing formulations (Figure 6). The rheological data suggested that incorporating Cloisite 15A leads to increased viscosity. Adsorption of the polymer chains over the organomodified MMT's surface results in such an observation. Natural, unmodified Cloisite Na^+ resulted in fragile structure formation (aggregate) isolated from each other without intercalation. Such an observation negates the presence of a 3D superstructure.[8d]

In the case of PSA, the viscoelastic characteristics, i.e., loss modulus (viscos response) and storage modulus (elastic responses), are important parameter to consider. During the bonding process (at low shear rate), the viscous component should be prevailing, whereas the elastic component should be dominating during the debonding process (at high shear rate). The oscillatory shear rheology can explain this property. Under sinusoidal shear, the shear stress of a viscous liquid and elastic solid can be expressed by eqs 8 and 9, respectively.

https://doi.org/10.1021/acsomega.1c05448
ACS Omega 2022, 7, 3844−3859

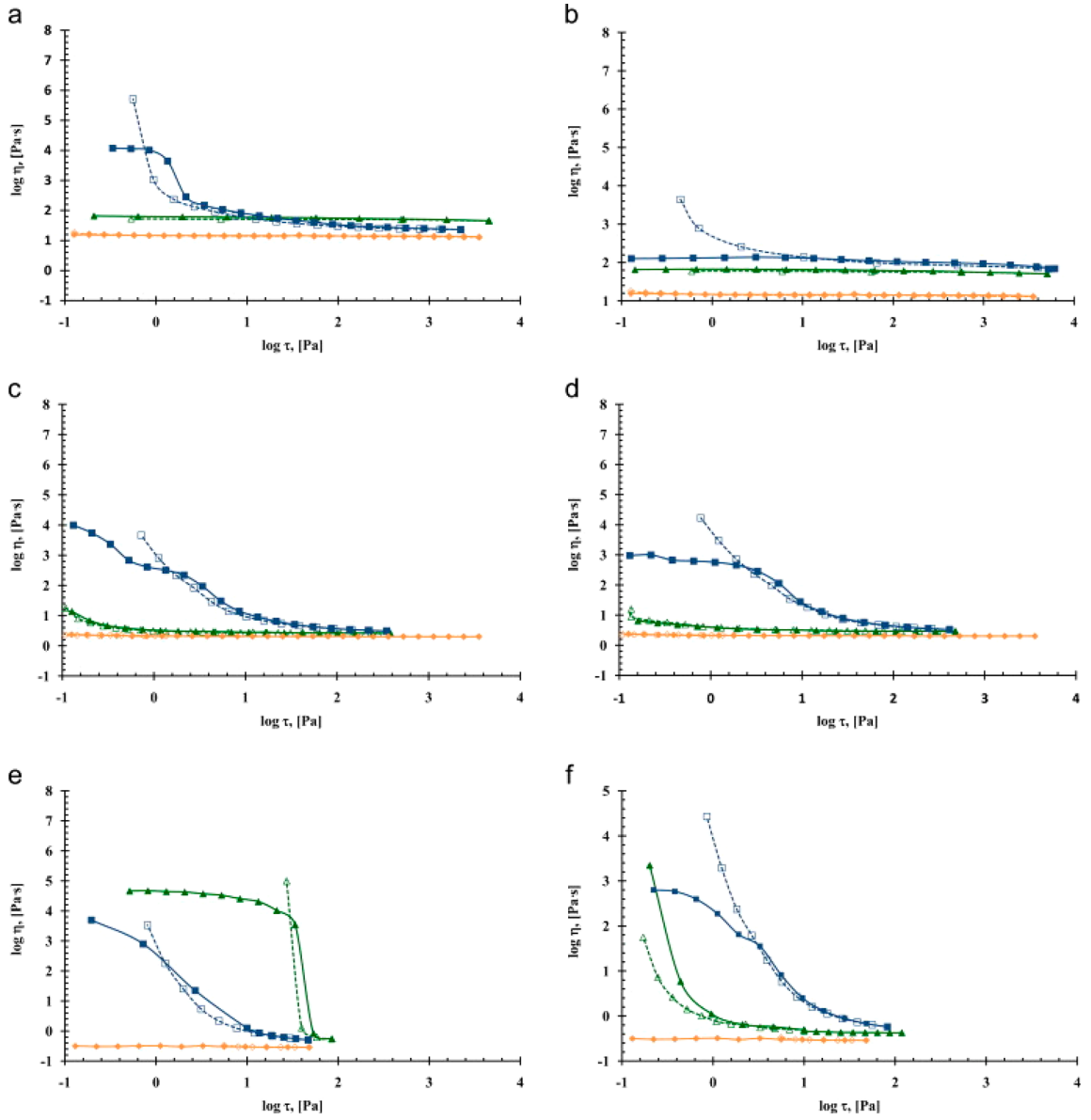

Figure 5. Graphical representation on viscosity of Cloisite Na^+ filled composite adhesive at 2 wt % (a, c, e) and 5 wt % (b, d, f) loading and at 20 °C (a, b), 40 °C (c, d), 60 °C (e, f). Green ▲ and blue ■ represents 0 and 4 min ultrasonication time, respectively. Gold ◆ indicates unfilled adhesive. Reprinted with permission from ref 8c. Copyright 2015 Elsevier.

$$\tau_{12} = \eta(\omega)\gamma_0\omega \cos \omega t \tag{8}$$

$$\tau_{12} = G(\omega)\gamma_0 \sin \omega t \tag{9}$$

The resultant shear stress of a viscoelastic liquid can be written as

$$\tau = G(\omega)\gamma_0 \sin \omega t + \eta(\omega)\gamma_0\omega \cos \omega t \tag{10}$$

where τ, G, γ_0, and ω represent shear stress, shear modulus, amplitude of shear strain, and angular frequency, respectively. The complex modulus can be obtained by dividing eq 10 by the strain amplitude (γ_0).

$$G^* = G(\omega) \sin \omega t + \eta\omega \cos \omega t \tag{11}$$

$$G' = G \tag{12a}$$

$$G'' = \eta\omega \tag{12b}$$

where G' and G'' are known as the storage and loss moduli, respectively. The ratio of loss modulus to storage modulus (G'/G'') gives tan δ (δ is the phase lag between stress and strain). The incorporation of NFs significantly impacts the storage and loss moduli. For instance, in a study, addition of cellulose nanocrystals (CNC) and functionalized cellulose nanocrystals (fCNC) in the acrylic PSA was investigated,[8e] where incorporation of CNC and fCNC showed lowering of G' at low frequency as compared to pristine PSA. This was attributed to the increase in the free volume of the polymer. However, due to a filler-reinforcing effect, the G' in the high frequency region was enhanced. A significant reduction in G' at low frequency region was observed with increased filler content, implying reduced entanglement or more mobility of the polymer chains and hence higher tack. Simultaneously, a noticeable increase in G'' at high frequency zone resulted in due to high energy dissipation during debonding process indicating higher peel strength.[8e]

https://doi.org/10.1021/acsomega.1c05448
ACS Omega 2022, 7, 3844−3859

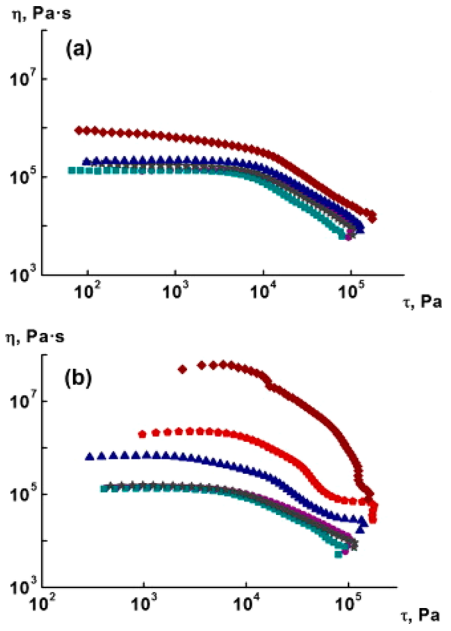

Figure 6. Graphical representation of viscosity of the Cloisite Na^+ (a) and Cloisite 15A (b) filled PIB-adhesive at 0% (purple ●), 5% (turquoise ■), 10% (gray ★), 20% (blue ▲), 30% (red ⬟), and 40% (maroon ◆) nanofiller loading. Reprinted with permission from ref 8d. Copyright 2016 Elsevier.

3.3. Curing. Curing kinetics are known to be impacted by the addition of filler. This is another guiding parameter to consider, as it determines the level of the adhesive's mechanical and adhesive properties. For instance, graphene oxide (GO), graphene oxide-ferric (GO-Fe), and graphene oxide-ferric dihydrogen phosphate (GO-Fe-P) hybrids NFs can significantly accelerate the curing reaction of room temperature curable one-part epoxy adhesive (EA) formulations. The curing mechanism is guided via a moisture-activated ketamine complex.[9] Typically, such processes are slow at room temperature. Curing efficiency was examined in terms of lap shear strength determination. The lap shear strength of EA increased from 0.33 to 4.57 MPa with an increase in the contact time from 5 to 24 h. When matched to EA, the lap shear strengths of GO/EA, GO-Fe/EA, and GO-Fe-P/EA were significantly higher under similar experimental conditions, typically, 1.67, 2.02, and 3.46 MPa, respectively, after 5 h of exposure and increased significantly as exposure time increased. When exposed for 24 h, samples of GO/EA, GO-Fe/EA, and GO-Fe-P/EA demonstrated higher adhesive strength of 8.01, 9.22, and 11.2 MPa, respectively. This was 75.3%, 102%, and 144% greater than neat EA. The functionalized GO nanocomposites were able to captivate moisture from the air. This promotes water molecules to drift from the surface to the bulk of the EA and, as a result, an acceleration in the decomposition rate of ketimine.[9]

3.4. Fracture Behavior. The mechanism associated with adhesive joint failure is a critical factor to consider the adhesive characteristics. The crack in the adhesive joint failure progresses through initiation and propagation. The crack propagation may occur either alongside with the adhesive-adherend interface (known as adhesion failure) or within the bulk of the adhesive (cohesive failure). The mechanism is dependent on the strength of the adhesive bond strength, fracture toughness, and the presence of microcracks in the adhesive. Some toughening mechanisms happen in the occurrence of large filler or aggregates. This process initiates crack deflection, crack pinning, microcracking, and matrix deformation, also known as the "micro" mechanism.[10a,b,3a] However, the nanofillers cannot deflect or pin the crack front; instead, they follow the "nano" pathway. This nano mechanism depends on the type of nanofiller structure used in the composition. The enhanced adhesion strength of the nanocomposite adhesive can be associated with the fracture toughness mechanisms such as, crack deviation, pull-out and crack bridging mechanism, depending on the geometry, length, surface modification, and flexibility of the NFs. Particle debonding is surmised to be a most critical toughening mechanism. Various other factors like plastic yielding or void enlargement (resulted by debonded particles) are also critical. Debonding of nanoclay and matrix shear banding are the critical energy degeneracy mechanisms happening at the nanoscale. This contributes to overall fracture toughness enhancements, especially in the case of clay based epoxy nanocomposites.[10c] Incorporation of nanotubes or nanofibers in adhesive exhibited crack bridging fracture toughness mechanism, which reduces the crack growth by reducing stress intensity near the crack tip. The crack deviation can be described by the roughness of fracture surfaces of nanocomposites. Rougher fracture surfaces require higher energy to develop in the course of crack growth. Moreover, high filler content also increases the rigidity of the system and leads to faster stress transfer throughout the material. The alignment of the nanoplatelets also influences the fracture energy, such as upright and parallel to the crack growth.

For example, Gholami et al.[10d] investigated the fracture behavior of the composite epoxy adhesive joint with randomly dispersed multiwalled carbon nanotubes (MWCNTs) and graphene oxide nanoplatelets (GONFs). The resulting composite demonstrated 82% and 155% increments in energy corresponding to a fracture, while the increment in the maximum load was 19% and 69%, respectively. Further alignment of the MWCNT and GONFs led to far higher improvements in the fracture energy initiation of 179% and 349% and a maximum load of 66% and 127%, respectively. The toughening mechanism was corroborated by the SEM studies on the surface yielded after fracture. The fractured surface obtained from the unfilled adhesive resulted in a smooth surface. It was conjectured that a brittle fracture mechanism with lower toughness was the predominant mechanism. The roughness of the fracture surface increases with the addition of a nanofiller. The results of MWCNTs nanocomposite adhesive indicated the presence of crack deflection, bridging, and pull-out. At higher nanofiller content, a reduction in fracture energy was observed due to agglomeration. By aligning MWCNTs in the direction perpendicular to the crack formation, the number of MWCNTs that experienced bridging and pull-out mechanisms was enhanced compared to the arbitrarily dispersed MWCNTs, thus showing higher fracture energy. Due to the higher surface area of GONFs compared to MWCTs, the former resisted crack growth. As a result, a crack tip pinning phenomenon was surmised to happen along with other mechanisms.

https://doi.org/10.1021/acsomega.1c05448
ACS Omega 2022, 7, 3844−3859

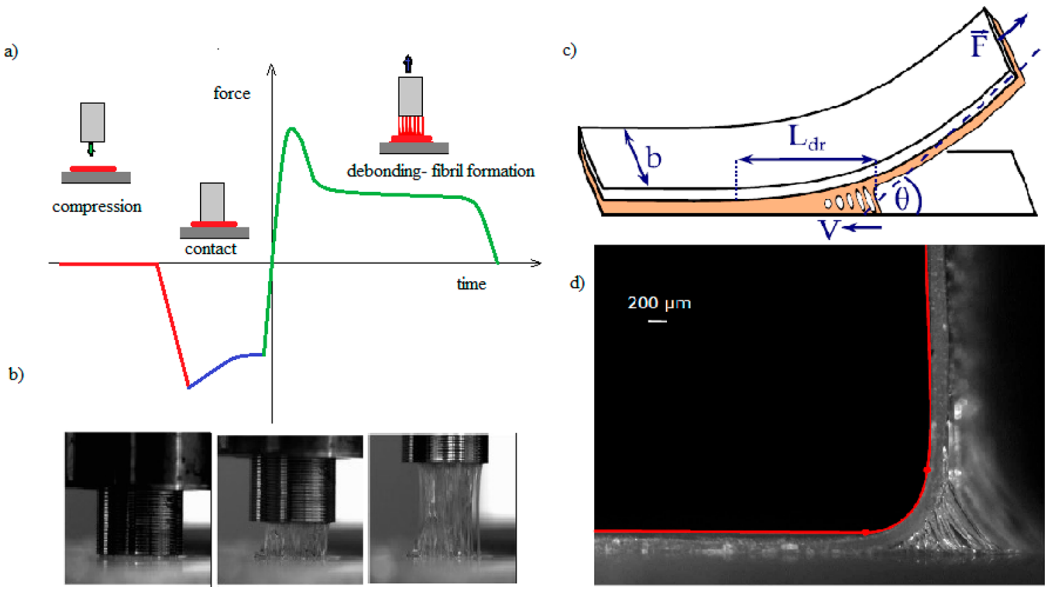

Figure 7. (a) Stress distribution curve for probe tack test of typical PSA. (b) Optical image of fibril formation during probe-tack analysis. Reprinted with permission from ref 11c. Copyright 2016 Elsevier. (c and d) Fibril formation during peel test. Reprinted with permission from ref 11d. Copyright 2020 Royal Society of Chemistry.

4. INFLUENCE OF NANOFILLERS ON ADHESION PROPERTIES

The two main types of NF-reinforced composite adhesive systems that can be considered for discussion are pressure-sensitive adhesives and structural adhesives. Moreover, the impact of the incorporation of NFs in the adhesive tack property of nonadhesive applications will also be considered. PSAs with both liquid and solid characteristics adhere to the substrate by applying mild pressure. On the other hand, structural adhesives are typically in the flowable form when applied at the joint. The full mechanical strength is attained once they hardened after the cross-linking reaction.

4.1. Pressure Sensitive Adhesives. The bond strength of PSA is contributed by the proper balance of viscous and elastic properties, which should satisfy the criteria to flow under low shear rates (bonding) and show elastic properties under high peel rates (debonding).[11a] According to Dahlquist,[11b] the criterion of tack, which stated that the elastic/storage modulus should be below 0.1 MPa to establish good contact on rough surface and a relatively large loss modulus should exhibit resistance against debonding. The adhesion strength of PSA is characterized by the tack, peel, and shear strength. In expressing the adhesion property of the materials, tack and peel tests are more trustworthy than shear tests. Both approaches rely heavily on flow and energy degeneracy (viscoelastic component) through bonding and debonding and vary in terms of contact time and force. It is worth noting that adhesives and bonded joints respond differently to peel and shear testing. Shear forces primarily focus on the adhesive's internal or cohesive strength, with a limited contribution of adhesion to the substrate. On the other hand, peel tests are more concerned with the bond strength between an adhesive and a substrate after applying pressure and the substrate has been wetted. Incorporating nanofiller on the PSA can increase the viscosity, requiring additional pressure to flow on the substrate. Increased viscosity and yield stress could improve the cohesive strength, consequently enhancing the PSA's shear strength. The presence of nanofillers has a significant impact on the cohesive strength and debonding processes at adhesive junctions. The failure of PSA joints occurs in numerous stages: the adhesive's homogeneous deformation, cavitation, fibril formation, and last fibril breakage (Figure 7).[11c,d] In general, incorporating different nanofillers improves the cohesiveness of nanofilled PSAs. This eliminates the cold flow. As a result, an increase in the shear resistance property is noted. However, this leads to a reduction in tack and peel strength as compared to unfilled one. It can be explained by the fact that very high cohesive strength may lead to excess hardening. As a result, the energy dissipation during the formation of a fibril is reduced. Moreover, the increase in the cohesive strength could only be observed when the thickness of the fibril formation is higher than the size of the nanofiller particles or their agglomerates.[12a] The comparable size of the fibril to that of the nanofiller/agglomerates size results in deteriorated mechanical properties. However, some investigations found the opposite effect, namely, improved peel and tack properties with a decrease in the shear resistance. To study such an effect, both isotropic and anisotropic nanofillers have been investigated in the adhesive matrix.

For instance, Khalina et al.[12b] studied about the use of 2 wt % silica nanoparticles in an adhesive composition. The base polymer was prepared by microemulsion polymerization of acrylic latex. The developed composite demonstrated improved tack and increased peel strength. However, the shear resistance value was found to decrease. This finding was most likely reached due to the emulsion-borne adhesive's heterogeneous nature, which did not have blatant connections amid discrete grains generated from the droplets of the emulsion. Based on the rheological results, an increase in the nanosilica volume fraction significantly increased the different moduli and impacted the rheology of the obtained polymer composite. As a result, a higher extent of inflow of energy is required to separate the adhesive layers from each other. This suggests that the two substrates are attached more effectively. The increase in tack strength was observed for silica 2% and

https://doi.org/10.1021/acsomega.1c05448
ACS Omega 2022, 7, 3844−3859

4% compared to an unfilled adhesive. This was due to the effective contact of the composite adhesive with the substrate due to the presence of silica particles. The peel strength initially increased (2% silica) compared to the blank but reduced by augmenting the silica content (4% silica). The high silica content would result in strong network formation, enhancing cohesion and reducing the peel strength (for 4% silica).[12b]

The debonding mechanism of PSA can also be explained from the probe tack curve by G_c/E relationship, as explained by Shull et al.,[13] where G_c is the critical energy release rate and E is Young's modulus. Three possibilities can be considered: In the first case, when the interfaces are particularly weak, debonding occurs due to low G_c/E, and thereby, crack propagates at the interface. After the maximum value is attained, there is a fast decline in the maximum debonding force until zero. In the second case, G_c/E may reach a point where it is comparable to the thickness of the adhesive layer. In this situation, the probe tack curves show an apparent plateau, fibrils start to form, and the tests resemble a tensile test. This is frequently noticed with strong, elastomeric adhesives. Finally, for the intermediary example, when G_c/E is higher than the size of the defect at the interface and lower than the layer thickness, a plateau decreases with increasing displacement.[13] Antonova et al. observed such a mixed debonding mechanism.[12a] They studied the influence of fumed silica Rosil-175 and halloysite nanotubes on the adhesion properties of PIB-based adhesive, which was dependent on various factors. The addition of 20% of Rosil increased the shear resistance (up to 2 orders) and slightly increased tack strength. However, the peel strength is almost the same as the unfilled one or varies depending on the adhesive thickness and peeling rate. Incorporation of halloysite showed a lower increase in the shear strength with much higher filler content (40%). This was attributed to the lower network strength. For composition containing 40 wt % halloysites, the tack properties did not alter significantly, but a 30−60% decrease in tack was observed for the thin-film. The peel strength of halloysite systems showed almost the same result as that of unfilled adhesive and increased up to 300% due to the translation of the mode of failure from the adhesive to cohesive mode.[12a]

The impact of incorporating filler on the adhesive property does not follow a generalized trend. Depending on the adhesive composition, it was observed that different categories of filler impacted the adhesion property differently. A few examples are discussed below.

4.1.1. Carbonaceous Nanofiller Based PSA Compositions. Very limited studies were explored utilizing carbonaceous fillers in PSA. Most of the works focused on the development of electrically conductive adhesive composition. It is expected that the incorporation of carbonaceous NFs such as graphene, carbon nanotubes (CNT), or carbon black into the adhesive system will improve the mechanical properties; however, it is worth mentioning that the adhesion properties (such as peel and tack strength) are reported to be compromised upon the addition of the NFs. Antosik et al. reported that the addition of graphene and CNT in the silicone PSA composition increased the electrical conductivity to 5.9×10^{-3} S/m and 1.4×10^{-1} S/m, respectively. However, the peel and tack strength were found to decrease with an increase in filler content. A pronounced effect was noted at a lower level of filler content. This was conjectured by the inventors due to the cross-linking of the adhesive.[12c] A similar result was observed for vinyl decorated modified graphene oxide (mGO)-filled UV curable acrylic PSA. The gel content of the composite adhesive was found to augment with an increase in the mGO content.[12d] As a result, the properties deteriorated. In the same way, incorporating nano carbon black and CNT in the acrylic PSA was found to significantly improve the shear strength (cohesion) with a drastic compromise in tack and peel strength.[12e]

4.1.2. Nanoclay-Based PSA Compositions. Brantseva et al.[8d] investigated the adhesive properties of PIB-based adhesive incorporating unmodified MMT Cloisite Na^+ and organo-modified (OMMT) Cloisite15A. The viscoelastic properties suggested that the 40 wt % Cloisite 15A increases the storage modulus, which dominates the loss modulus. Consequently, a significant rise in holding time was observed. Cloisite Na^+ forms stiff aggregates within the adhesive matrix without intercalation. In this situation, the aggregates operate as stress concentrators and thus just allowed a modest improvement in the holding time and only for the 40 wt % Cloisite Na^+ filled adhesive. Considering thin films, incorporation of fillers resulted in a significant decrease in the debonding energy in the probe tack test (60% for unmodified clay and 78% for organomodified clay), which is typical for increased cohesive strength. In the case of thick film debonding energy, unfilled PIB shows an almost similar result, due to the development of a mechanical network that allowed enhanced energy degeneracy through the entire thickness. A 2-fold increment in the peel strength was noted with the incorporation of 10 wt % Cloisite 15A in the thin film. A further increase in the filler loading decreased the peel resistance due to the worsening effect of the adhesive joint. When the amount reached 40%, the elastic and peel strength increased. As a result, a mixed-mode failure mechanism took place. On the contrary, a monotonous growth of peel resistance was observed in the case of a thick film. Therefore, it can be concluded that peel, tack, and shear properties are prejudiced by the kind, content of clay particles, and thickness of the adhesive.[8d]

Moghadam et al.[14a] reported about the adhesion attributes of modified MMT (Cloisite 15A modified with dimethyl dihydrogenated-tallow quaternary ammonium salt; C15A) reinforced poly(butyl acrylate-*co*-vinyl acetate-*co*-acrylic acid) based nanocomposite PSA developed via in situ emulsion polymerization. The authors observed a significant increase in the various adhesion parameters by adding 1 wt % C15A. This is due to the increase in the entanglement density of the PSA. However, further increases in the filler volume fraction lowered the peel and tack properties. Maximum peel and probe tack were obtained for the PSA containing 1 wt % C15A along with 0.25 wt % chain transfer agent (CTA). The addition of a small amount of C15A without CTA showed a high increase in shear resistance. The increased molecular weight and better interaction between the polymer chain and organoclay increased the shear viscosity and cohesive strength. The rise in entanglement density and molecular weight of the PSA nanocomposite with 1 wt % C15A contributed to the viscoelastic energy dissipation factor. This resulted in the improvement of the peel strength. The rise in polydispersity index simultaneously amplified the quantity of low molecular weight materials with strong chain mobility, thus increasing the probe tack. A further increase in the nanoclay to 1.5 wt % resulted in the agglomerate formation, thereby decreasing the peel strength and probe tack.[14a]

https://doi.org/10.1021/acsomega.1c05448
ACS Omega 2022, 7, 3844−3859

4.1.3. Oxide Containing Nanofiller Based PSA Compositions. Reports relating to the use of nano-oxide based PSA composition with an improved adhesion property is far and few. Very limited research work has been explored. Zhang et al. utilized nano-SiO_2 and nano-Al_2O_3 into silicone PSA to achieve high heat resistance. The adhesive property indicated that the peel strength increased whereas the tack strength reduced with an increase in the NF content.[14b]

4.2. Structural Adhesive. Adhesively bonded joints are gaining popularity as mechanical joint alternatives in engineering applications as they offer several advantages over traditional mechanical seals. The influence of NFs on the improvement of the mechanical properties including tensile strength, stiffness, shear strength, and typical adhesion properties including lap shear strength, peel strength (180° peel test, 90° peel test), and tack (probe tack, loop tack) were experimentally investigated by many researchers. A few of them are captured in this section that is segmented based on the types of filler used.

4.2.1. Carbonaceous Nanofiller Based Adhesive Compositions. Khan et al.[15] reported about the impact of solution exfoliated graphene on the adhesive property of polyvinyl acetate (PVAc) adhesive. They prepared high concentration solutions of PVAc in tetrahydrofuran with and without various concentrations of graphene ranging from 0.2 to 3 wt %. This coating was applied on wood pieces, and the tensile and shear properties were measured. The result indicated better adhesion properties. The stiffness was found to be increased by 50% while the tensile strength increased by 100% due to the incorporation of 0.1 vol % graphene. The results were compared against the pristine polymer (as shown in Figure 8). The graphene addition increased the polymer's stiffness, leading to cavity formation and fibril resisting deformation at higher stress.[15]

Similarly, Tounici et al.[16] studied the effect of the addition of oxidized graphene (GO) on the adhesive properties of waterborne polyurethane urea dispersions (PUDs). The adhesion strength of plasticized poly(vinyl chloride) (PVC)/PUD/plasticized PVC joints was raised by adding 0.02−0.04 wt % GO (measured via T-peel test), whereas the strength of stainless steel/PUD/stainless steel joints was increased by adding 0.05−0.10 wt % GO (measure via single lap-shear). The increased adhesion strength of nanocomposite adhesive can be attributed to the formation of covalent interaction amid surface functionalities on the nanoparticles and the isocyanate group. The grafted GO sheets were incorporated between the polymer chains during the phase inversion. This resulted in the segment separation (hard and soft) of the polymer matrix. Beyond the 0.4 wt % GO, a few GO particles could not form such covalent bonds, thus remaining trapped between the polyurethane urea chains, resulting in decreased peel strength. In the case of PVC/PUD adhesive joint containing 0.01−0.04 wt % GO, the cohesive failure mainly occurred, indicating excellent adhesion.[16]

Due to nanomaterials' poor dispersibility and solubility in solvents, incorporating such materials into the polymer matrix becomes very difficult. Surface modification with organic functional molecules improves the dispersion into the polymer matrix by better wetting nanoparticles with polymer chains. It leads to improved mechanical and adhesion properties due to covalent interaction between nanoparticles and the polymer matrix. Such modification was carried out by Mondal et al.[17] using the "grafting to" approach to establishing covalent attachment between carboxylated graphene platelets and

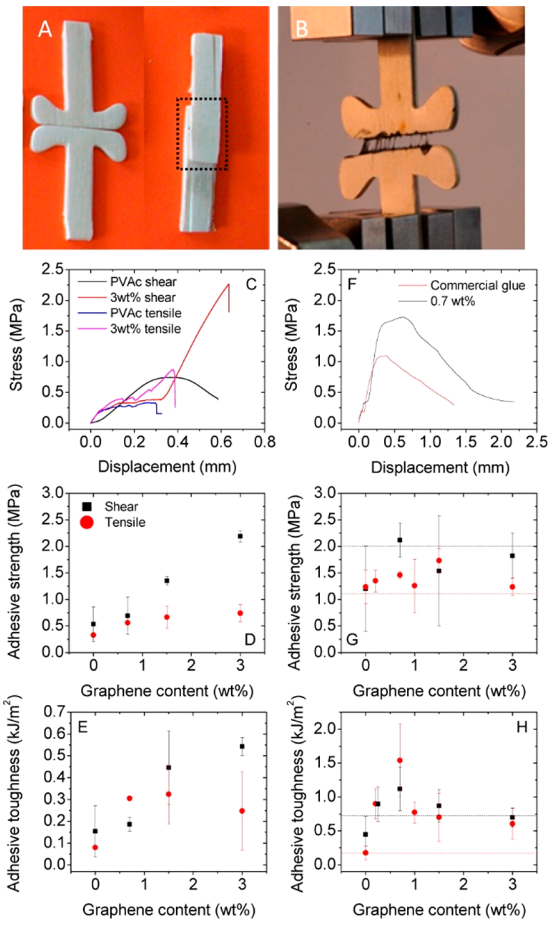

Figure 8. Adhesive characteristics of PVAc/graphene adhesive. (A) Test samples images for tensile test (left) and shear test (right). (B) Image of tensile testing. (C) Plot of tensile and shear stress of prepared PVAc adhesive vs displacement. (D) Influence of graphene content on the tensile and shear properties, and (E) toughness for the prepared PVAc adhesives. (F) Tensile property of unfilled and graphene-filled commercial adhesive. (G) Influence of graphene content on the tensile and shear properties and (H) toughness for the commercial adhesives. The untreated glues are represented by dotted lines. Reprinted with permission from ref 15. Copyright 2013 American Chemical Society.

silane-based polymers (SG). The modified SG was compared with the system formed by the physical mixing of unmodified graphitic platelets and silane polymer (SUG). This high-performing nanocomposite exhibited an instant conducting adhesive characteristic eliminating the requirement of an external cross-linking agent. The carboxylated graphene platelets (XG) were subjected to [3-(2-aminoethylamino)-propyl]- trimethoxysilane (AEPT) monomer in the presence of a catalytic amount of *N,N′*- dicyclohexylcarbodiimide (DCC) via a tetrahedral intermediate and proton transfer reaction as shown in Figure 9. Further, monomer grafted XG underwent a polycondensation reaction under moisture conditions to form SG. The formation of SG was thermodynamically more favorable due to the large surface area and greater heat liberation of polymer grafted nanomaterials, resulting in a higher enthalpy contribution than SUG. The fracture surface analysis suggested that SG formed a hierarchical array of nanoplatelets inside the polymer matrix. A single lap-shear test tested the adhesion properties of the composite adhesive for the different substrates glass and canvas. Cohesive failure was

https://doi.org/10.1021/acsomega.1c05448
ACS Omega 2022, 7, 3844−3859

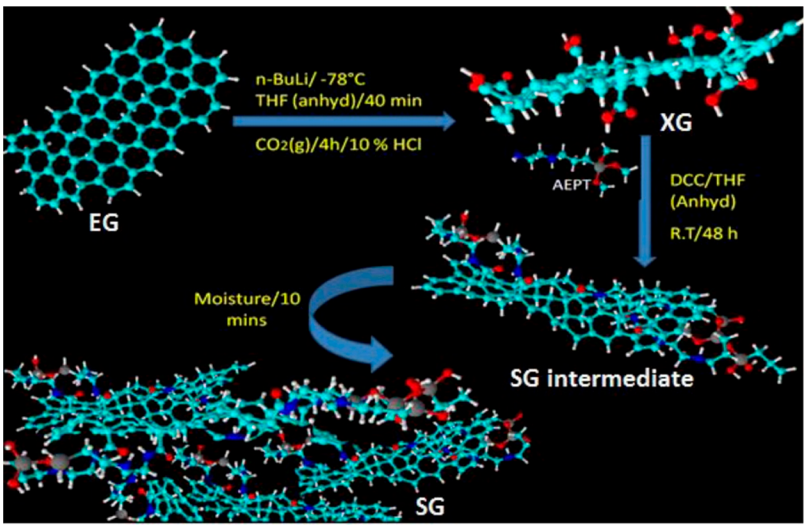

Figure 9. Proposed reaction scheme for creating SG from XG with the help of DCC coupling agent. Reprinted with permission from ref 17. Copyright 2014 American Chemical Society.

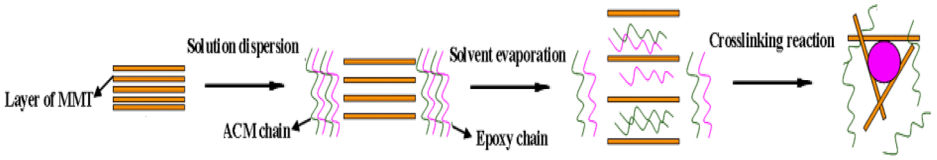

Figure 10. Nanoclay dispersion in the epoxy-acrylic rubber (ACM) blend via solvent mixing followed by a final nanocomposite adhesive via cross-linking. Reprinted with permission from ref 18. Copyright 2014 Elsevier.

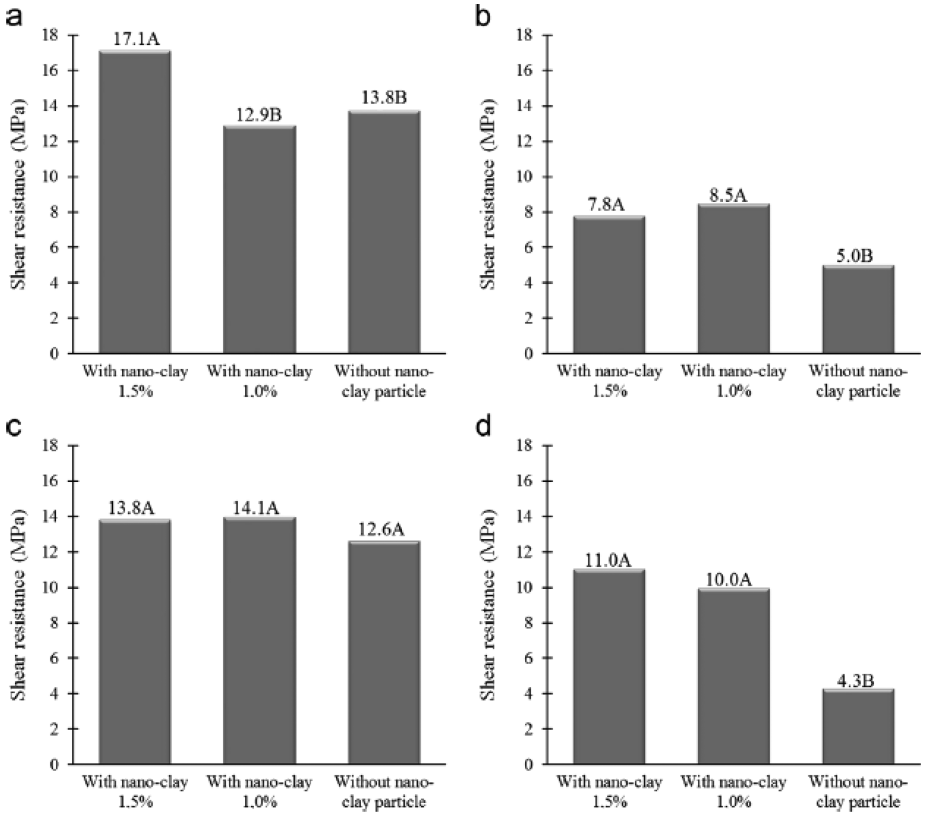

Figure 11. Representation of shear resistance in dry and wet conditions: (a) PVAc-nanoclay (dry), (b) PVAc-nanoclay (wet), (c) UF-nanoclay (dry), and (d) UF-nanoclay (wet). Reprinted with permission from ref 20. Copyright 2015 Elsevier.

https://doi.org/10.1021/acsomega.1c05448
ACS Omega 2022, 7, 3844−3859

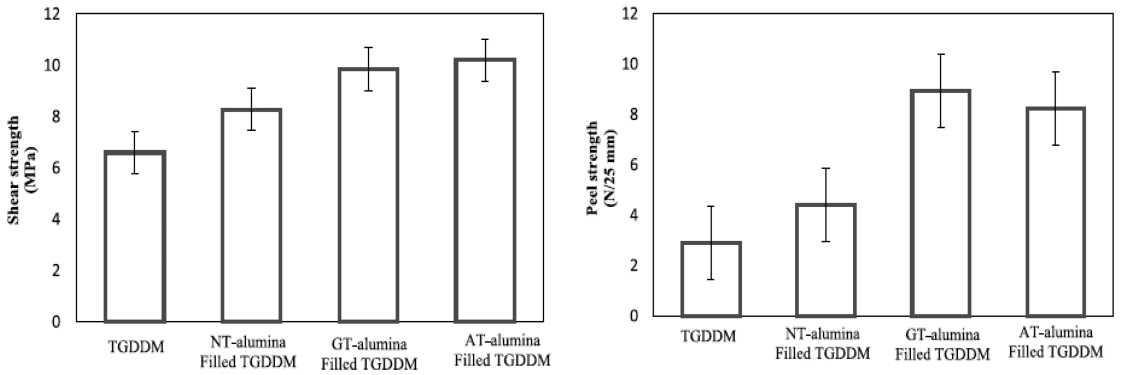

Figure 12. Lap-shear and peel strength of various nanocomposite adhesives. Reprinted with permission from ref 22. Copyright 2019 Elsevier.

observed for the glass surface due to the greater affinity of the silane polymer toward the glass. Whereas, increased lap-shear strength was observed for SG (1250 N/m^2) as compared to SUG (1121 N/m^2) and PAEPT (1086 N/m^2) due to the increased covalent interaction of SG over SUG when tested on canvas sample.[17]

4.2.2. Nanoclay Based Adhesive Compositions. The combined impact of montmorillonite (MMT) on the adhesive properties and micromorphologies of epoxy/acrylic rubber (ACM) blend adhesive film was investigated.[18] The complete separation in the phase structure and a higher T_g of epoxy in the epoxy/ACM/MMT nanocomposites were noted. This was due to the catalytic effect of MMT on the curing of the polymer, which allowed them to form an agglomerate and reduced sizes and augmented the epoxy domains in the ternary nanocomposites. ACM and epoxy chains penetrated the clay layers during the solution blending process of all the components. After the solvent loss, the intercalated state of MMT and after cross-linking of the epoxy region resulted in complete separation of the layered filler, as shown in Figure 10.

The mechanical study showed a concomitant effect of nanoclay on both the toughness and tensile moduli of the epoxy/ACM blend, which was due to the small domain sizes and unique interface of MMT-clay in the nanocomposites. The maximum increment in adhesive strength was observed for 3% clay incorporated nanocomposite compared to the binary blend without clay.[18] Incorporating nanosilicate in natural rubber latex (NRL) based adhesive can significantly improve the peel strength. The increase in peel strength level varied depending on the type of nanoclay (aspect ratio, interlayer distance) and its loading. The improved cohesive strength of nanocomposite NRL adhesive is due to improved rubber−nanosilicate interaction.[19]

The adhesion strength and percent of wood failure of nanoclay modified polyvinyl acetate (PVAc) and urea-formaldehyde (UF) adhesives were investigated by Moya et al.[20] The highest adhesive strength was noted for PVAc adhesive with 1.5 wt % nanoclay addition under dry conditions due to better polymer−clay interactions. Nanoclay addition improved the lap shear strength for both the adhesive under wet conditions (Figure 11). Under wet conditions, nanoclay incorporation improved the percentage of wood failure, which is due to a percolation phenomenon between the nanoclay particles. This connected infinite cluster structure of nanoclay improves the adhesive properties.[20]

4.2.3. Oxide Containing Nanofiller Based Adhesive Compositions. Lap joint characteristics of two different metals, mild steel and aluminum, by nano TiO_2 filled epoxy adhesive were investigated by Ghosh et al.[21] It was found that bond line thickness increased with increasing filler amount attributed to the adhesive's rheological behavior and viscoelastic properties, providing higher resistance to flow. TiO_2 nanofiller epoxy-based composite adhesive showed superior results over the use of neat epoxy glue, with an optimal level of 10 wt % of TiO_2. The lap shear strength of the 10 wt % TiO_2 nanofiller composite adhesives was also maintained at increased temperatures up to 150 °C.[21]

On a different note, Tutunchi et al.[4] reported the impact of the various amount of Al_2O_3-nanoparticle on the adhesion strength of steel− epoxy composite joints adhered with two-component structural acrylic adhesive. The inclusion of an optimum dose of nano-Al_2O_3 (1.5 wt %) resulted in increased shear (∼43%) and tensile strength (∼63%). This was due to effective stress distribution between the fillers and the polymer. However, further addition of nanoparticles leads to decreased properties. Up to a certain level of nanoparticles addition effectively fill all the microscopic gaps present in the polymers matrix, thus achieving maximum contact between the filler and the adhesive. However, beyond this limit, poor matrix infiltration occurs due to the insufficient interaction of nanoparticles with the adhesive. Additionally, viscosity became so high that it restricted efficient degassing. Degassing is a critical step to remove the dissolved gases in the matrix. The presence of such gases might lead to the formation of bubbles during the application of the adhesives. The addition of nanoparticles reduced the peel strength, which can be attributed to the reduced mobility of the polymer chain and increased T_g.[4]

The influence of Al_2O_3, SiO_2, and TiO_2 nanoparticles on the adhesion strength of steel joints bonded using two-part structural acrylic adhesives was investigated in another study.[7c] The result indicated that the maximum impact was provided by nano-Al_2O_3, which increased both shear and tensile adhesion by 43% and 63%, respectively. Composite adhesive with SiO_2 and TiO_2 nanoparticles showed comparable adhesion strength. This improvement was due to better stress transmission between the fillers and adhesive matrix, which allowed a larger local plastic deformation of the matrix. A decrease in peel strength of nanocomposite adhesive was observed due to the reduction in chain mobility and increase in T_g and brittleness.[7c]

Surface modification of NFs tends to improve the dispersion of the filler in the adhesive matrix. The effects of different silane-modified nano alumina on the adhesive properties of epoxy (TGDDM) nanocomposite adhesive were investigated by Maghsoudian et al.[22] Aminopropyltrimethoxysilane (APS)

https://doi.org/10.1021/acsomega.1c05448
ACS Omega 2022, 7, 3844−3859

treated alumina (AT-alumina) and 3-glycidoxypropyltrimethoxysilane (GPS)-treated alumina (GT-alumina) along with nontreated nanoalumina were dispersed ultrasonically and incorporated into the adhesive system via in situ polymerization. The higher heat of cure and high cross-linking density of all the nanocomposite adhesive obtained due to the catalytic interaction of functional groups such as hydroxyl groups on NT-alumina nanoparticles and the NH_2 amine group on the AT-alumina with an oxirane ring of the epoxy resin. Additionally, the oxirane group present on GT-alumina nanoparticles took part in the curing reaction. Adhesion strengths are shown in Figure 12. Silane modified NFs showed higher shear strength indicating better interaction between NFs and the matrix. The GT-Alumina nanocomposite attained the highest peel strength, which can be attributed to higher energy dissipation during crack propagation and better toughness.[22] Similarly, incorporating highly polar nanoparticles SiO_2 into a hydrophobic polymer leads to poor dispersion and adhesive properties due to the formation of aggregate in the matrix. Silane coupling agents have traditionally been utilized to change the surface characteristics of SiO_2 NFs to solve this problem. Heo et al.[23] reported the impact of various modified silanized SiO_2 NFs on the adhesive properties of epoxy adhesives. SiO_2 nanoparticles were synthesized via the sol−gel method, and their surface was modified by different coupling agents such as (3-glycidoxypropyl) methyldiethoxysilane (GPTMS) and (3-amino-propyl) trimethoxysilane (APTMS). Different characterization analysis indicated the presence of chemical cross-linking of hardener (TETA) on GPTMS treated epoxy-functionalized NF (EPOXY-NF) after curing. Similarly, epoxy resin was found to be chemically cross-linked on the APTMS treated amine-functionalized NF (NH_2-NF). The shear strength of adhesives composed of TETA hardener/EPOXY-NF and DGEBA resin/NH_2-NF showed 79% and 49% increments, respectively, compared to unmodified SiO_2 based adhesive.[23]

4.3. Nonadhesive. Autohesive tack properties of a typical elastomer are highly essential for tire or rubber industries, as it facilitates easy fabrication of multicomponent rubber compounding. The tack between two unvulcanized rubber is termed autohesive tack due to the interdiffusion of the elastomeric chain across the polymer−polymer interface. It is worth mentioning that the addition of nano reinforcing filler can increase the tack strength of the elastomer. A unique mechanism was explained by Basak et al.[24] to understand the role of nanoclay in the bonding-debonding during tack test of an unvulcanized EPDM rubber in terms of green strength, creep compliance, molecular entanglement weight, relaxation time, the self-diffusion coefficient, and the monomer friction coefficient (ζ_0). Tack test was performed by placing two samples together at one end under load, measuring the pull-off force required to separate those strips after sufficient contact time. The composite EPDM showed 137% higher tack strength as compared to neat EPDM by adding 4 phr nanoclay (MMT-Cloisite- Na^+), whereas further addition resulted in decreased tack strength. Because of the reinforcing activity of the nanoclay in the EPDM matrix, there was a simultaneous improvement in green strength and a reduction in creep compliance (contact flow) of EPDM rubber. The high green strength can restrict contact flow and diffusion of the polymer chain across the interface, thus reducing the tack strength, but EPDM composite showed an opposite trend. This was because the increase in green strength dominated over the decrease in contact flow. This decline in contact flow was so small that sufficient contact and diffusion across the interface can still be achieved. The reduction in tack strength happened when the decrease in contact flow dominated over the increase in green strength. That was observed for higher clay loading (>4 phr). Further addition of nanoclay resulted in the aggregate formation and reduced polymer−polymer contact and chain mobility at the interface, thus reducing the tack strength. Moreover, at 4 phr clay loading, the diffusion of elastomer chains across the interface was sufficient to form entanglements. The entangled chains had a higher monomer friction coefficient value, making them more resistant to separation. As a result, the tack strength improved.[24] Similarly, the influence of sepiolite nanoclay on the autohesive tack strength of brominated isobutylene-*co*-p-methylstyrene (BIMS) rubber was conducted by Kumar et al.[25] The incorporation of 8 phr nanoclay enhanced the tack strength of BIMS by 300% as compared to neat BIMS. The increment of the tack strength of nanocomposite rubber can be explained similarly as above.

5. CONCLUSIONS

The utilization of nanomaterials in advanced adhesive technology to achieve maximum adhesive properties is described in this review. The best adhesion properties can be achieved only when the NFs are uniformly dispersed with improved filler−matrix interaction. The dispersion can be controlled by adopting the dispersion technique and via appropriate surface modification of NFs. The in situ polymerization process for nanofiller distribution and ultrasonic mixing technique were found to be the most efficient methods to obtain uniform dispersion. Moreover, for a sheet like nanofiller such as nanoclay or graphene, exfoliation or intercalation of the nanofiller is essential to achieve the best result, which is in general obtained from an optimum filler loading, resulting in improved cohesive strength and modulus of the adhesive with reduced residual stress. Higher filler content leads to aggregate formation, acting as a stress concentration point at the joint thus worsening the joint strength. The incorporation of modified NFs not only improves the compatibility between NFs and the matrix but also contributes to the curing kinetics and rheology that have a significant impact on the adhesive property. NFs also improve the wetting property, which is essential for strong adhesion. The fracture toughening of the nanocomposite during adhesive joint failure can follow various mechanisms depending on the geometry of the NFs, surface modification, and flexibility of the NFs. The crack-bridging and crack deviations are the most common toughening mechanism observed in the nanocomposite-adhesive to reduce the crack propagation. NFs incorporation contributes to the increase in cohesive strength of the adhesive, which increases the shear resistance (increased holding time for PSA), which usually reduces the peel and tack strength, but the opposite trend is also observed in many cases. The impact of adding NFs in the structural and PSA adhesive on the shear resistance, peel strength, and tack strength depends on the nature of the individual filler and adhesive system, filler−matrix interaction (covalent bond formation, elastic network, and chain adsorption on the NFs surface), and defect and failure mechanisms. The inclusion of NFs in the rubber system improved the autohesive tack property. In most of the cases, the aim of incorporating carbonaceous NFs in the adhesive system especially in PSA is carried out to achieve improved electrical conductivity that in general compromises with their

https://doi.org/10.1021/acsomega.1c05448
ACS Omega 2022, 7, 3844−3859

adhesive properties. Developments of new strategies to simultaneously improve specific properties and adhesion strength is still a challenge for future generations. However, the impact of NFs size and shape on the composite adhesive strength is barely studied by the researchers, which can be a broad area of research in future adhesive technology.

AUTHOR INFORMATION

Corresponding Authors

Santanu Chattopadhyay − *Rubber Technology Centre, Indian Institute of Technology, Kharagpur, West Bengal, India 721302*; Email: santanu@rtc.iitkgp.ac.in

Titash Mondal − *Rubber Technology Centre, Indian Institute of Technology, Kharagpur, West Bengal, India 721302*; orcid.org/0000-0003-0825-6337; Email: titash@rtc.iitkgp.ac.in

Authors

Aparna Guchait − *Rubber Technology Centre, Indian Institute of Technology, Kharagpur, West Bengal, India 721302*

Anubhav Saxena − *R&D, Pidilite Industries Limited, Mumbai 400059, India*; orcid.org/0000-0002-3113-4197

Complete contact information is available at: https://pubs.acs.org/10.1021/acsomega.1c05448

Notes

The authors declare no competing financial interest.

Biographies

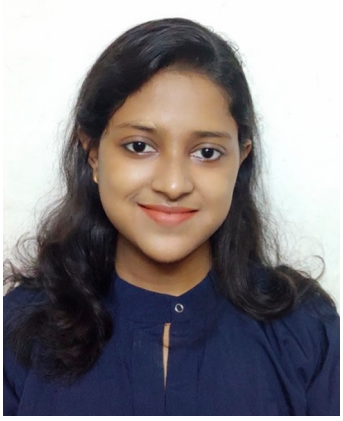

Aparna Guchait received her M.Tech. degree in Polymer Engineering and Technology from the Institute of Chemical Technology, Mumbai, India, in 2020. She is currently pursuing a Ph.D. at the Indian Institute of Technology, Kharagpur, India. Her research interest is focused on the development of biobased adhesives for different applications.

Anubhav Saxena is an innovation specialist with 20 years of diverse research experience. He owns 50+ patents and authored 40+ articles, reviews, highlights, and book chapters. Currently, Anubhav is the R&D President at Pidilite Industries. He is a Fellow of the Royal Society of Chemistry (FRSC) and on the Advisory Board of the American Chemical Society's flagship magazine *CE&N* and *ACS Omega* and *ACS Chemical Health & Safety* journals.

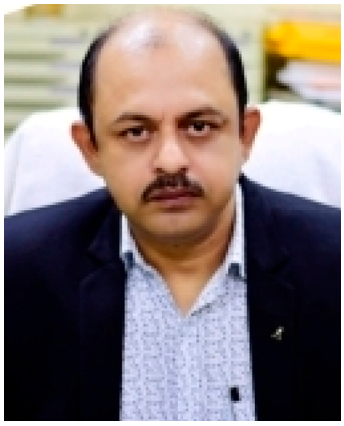

Santanu Chattopadhyay is currently a Professor and Head of the Rubber Technology Centre, Indian Institute of Technology Kharagpur, India. He has been serving there as a faculty member since 2004. Prof. Chattopadhyay pursued his postdoctoral research work at the Georgia Institute of Technology, from the Chemical Engineering Department. Prior to that, he did his postdoctoral studies as well at the University of Western Ontario, Canada. Prof. Chattopadhyay earned his Ph.D. from IIT Khargpur on electron beam irradiated TPE blends as shape-memory materials. Prior to these, he earned his M.Tech. (Materials Science) and M.Sc. (Chemistry) from IIT Bombay and IIT Kharagpur, respectively. His research interests include green rubbers and compounds, viscoelasticity, and processing of rubbers, rubber based biomaterials, soft energy materials, die and mold design and simulation, and design of rubber products.

Titash Mondal received his B.Sc. and M.Sc. in Chemistry from the University of Calcutta, India. Following this, he received his M.Tech. degree in 2011 in Rubber Technology from the Indian Institute of Technology Kharagpur, India. He got his Ph.D. degree in 2015 jointly from the Indian Institute of Technology of Patna, India, and University of Houston, U.S., under the joint guidance of Prof. Anil K. Bhowmick and Prof. Ramanan Krishnamoorti. From 2016 to 2020, he worked as a Scientist in the U.S.-based silicone industry. Since 2020, he has been working as an Assistant Professor at the Indian Institute of Technology Kharagpur, India. His expertise focuses on the

https://doi.org/10.1021/acsomega.1c05448
ACS Omega 2022, 7, 3844−3859

development of composites based on soft materials and printed electronics.

■ ACKNOWLEDGMENTS

T.M. acknowledges generous support of the ISIRD funding (Grant IIT/SRIC/RT/ESA/2020-2021/081) from IIT Kharagpur, India.

■ REFERENCES

(1) (a) Saha, S.; Mondal, T.; Bhowmick, A. K. Pressure Sensitive Adhesive for Healthcare Applications. In *Reference Module in Materials Science and Materials Engineering*; Elsevier, 2021; DOI: 10.1016/B978-0-12-820352-1.00106-1. (b) Raihan, R.; Elenchezhian, M. R. P.; Vadlamudi, V. Chapter 11- Durability of bonded composite systems. In *Durability of Composite Systems*, 1st ed.; Woodhead Publishing Series in Composites Science and Engineering; Reifsnider, K. L., Ed.; Elsevier, 2020; pp 383−401. (c) Ebnesajjad, S.; Landrock, A. H. Chapter 4: Classification of adhesives and compounds. In *Adhesives Technology Handbook*, 3rd ed.; Ebnesajjad, S., Landrock, A. H., Eds.; Elsevier, 2014; pp 67−83. (d) Schultz, J.; Nardin, M. Chapter 3: Theories and Mechanisms of Adhesion. In *Handbook of Adhesive Technology*, revised and expanded, 2nd ed.; Pizzi, A., Mittal, K. L., Eds.; Marcel Dekker Inc.: New York, 2003; pp 53−68.

(2) (a) Brantseva, T. V.; Antonov, S. V.; Gorbunova, I. Y. Adhesion Properties of the Nanocomposites Filled with Aluminosilicates and Factors Affecting Them: A Review. *Int. J. Adhes. Adhes.* **2018**, *82*, 263−281. (b) Frigione, M.; Lettieri, M. Recent Advances and Trends of Nanofilled/Nanostructured Epoxies. *Materials (Basel)* **2020**, *13* (15), 3415. (c) Osman, M. A.; Mittal, V.; Morbidelli, M.; Suter, U. W. Polyurethane Adhesive Nanocomposites as Gas Permeation Barrier. *Macromolecules* **2003**, *36* (26), 9851−9858. (d) Prolongo, S. G.; Gude, M. R.; Ureña, A. Chapter 3: Nanoreinforced Adhesives. In *Nanofibers*; Kumar, A., Ed.; Intec, 2010; pp 39−68. (e) Gokul Ganesh, M.; Lavenya, K.; Kirubashini, K. A.; Ajeesh, G.; Bhowmik, S.; Epaarachchi, J. A.; Yuan, X. Electrically Conductive Nano Adhesive Bonding: Futuristic Approach for Satellites and Electromagnetic Interference Shielding. *Adv. Aircr. Spacecr. Sci.* **2017**, *4* (6), 729−744.

(3) (a) Fu, S. Y.; Feng, X. Q.; Lauke, B.; Mai, Y. W. Effects of Particle Size, Particle/Matrix Interface Adhesion and Particle Loading on Mechanical Properties of Particulate-Polymer Composites. *Compos. Part B Eng.* **2008**, *39* (6), 933−961. (b) Camargo, P. H. C.; Satyanarayana, K. G.; Wypych, F. Nanocomposites: Synthesis, Structure, Properties and New Application Opportunities. *Mater. Res.* **2009**, *12* (1), 1−39.

(4) Tutunchi, A.; Kamali, R.; Kianvash, A. Effect of Al2O3 Nanoparticles on the Steel-Glass/Epoxy Composite Joint Bonded by a Two-Component Structural Acrylic Adhesive. *Soft Mater.* **2016**, *14* (1), 1−8.

(5) (a) Jojibabu, P.; Zhang, Y. X.; Prusty, B. G. A Review of Research Advances in Epoxy-Based Nanocomposites as Adhesive Materials. *Int. J. Adhes. Adhes.* **2020**, *96*, 102454. (b) Bhattacharya, M. Polymer Nanocomposites-A Comparison between Carbon Nanotubes, Graphene, and Clay as Nanofillers. *Materials (Basel).* **2016**, *9* (4), 262. (c) Rane, A. V.; Kanny, K.; Abitha, V. K.; Thomas, S. *Methods for Synthesis of Nanoparticles and Fabrication of Nanocomposites*; Elsevier Ltd., 2018. (d) Mondal, T.; Ashkar, R.; Butler, P.; Bhowmick, A. K.; Krishnamoorti, R. Graphene Nanocomposites with High Molecular Weight Poly (ε -Caprolactone) Grafts : Controlled Synthesis and Accelerated Crystallization. *ACS Macro Lett.* **2016**, *5* (3), 278−282. (e) Mondal, T.; Basak, S.; Bhowmick, A. K. Ionic Liquid Modification of Graphene Oxide and Its Role towards Controlling the Porosity, and Mechanical Robustness of Polyurethane Foam. *Polymer (Guildf)* **2017**, *127*, 106−118.

(6) (a) Yu, H. Y.; Qin, Z. Y.; Yan, C. F.; Yao, J. M. Green Nanocomposites Based on Functionalized Cellulose Nanocrystals: A Study on the Relationship between Interfacial Interaction and Property Enhancement. *ACS Sustain. Chem. Eng.* **2014**, *2* (4), 875−886. (b) Li, F.; Yu, H.-Y.; Li, Y.; Hussain Abdalkarim, S. Y.; Zhu, J.; Zhou, Y. "Soft-rigid" Synergistic Reinforcement of PHBV Composites with Functionalized Cellulose Nanocrystals and Amorphous Recycled Polycarbonate. *Compos. Part B Eng.* **2021**, *206*, 108542. (c) Yu, H. Y.; Chen, R.; Chen, G. Y.; Liu, L.; Yang, X. G.; Yao, J. M. Silylation of Cellulose Nanocrystals and Their Reinforcement of Commercial Silicone Rubber. *J. Nanoparticle Res.* **2015**, *17*, 361.

(7) (a) Khalil, N. Z.; Johanne, M. F.; Ishak, M. Influence of Al_2O_3 Nanoreinforcement on the Adhesion and Thermomechanical Properties for Epoxy Adhesive. *Compos. Part B Eng.* **2019**, *172*, 9−15. (b) Dorigato, A.; Pegoretti, A.; Bondioli, F.; Messori, M. Improving Epoxy Adhesives with Zirconia Nanoparticles. *Compos. Interfaces* **2010**, *17* (9), 873−892. (c) Yadollahi, M.; Barkhordari, S.; Gholamali, I.; Farhoudian, S. Effect of Nanofillers on Adhesion Strength of Steel Joints Bonded with Acrylic Adhesives. *Sci. Technol. Weld. Join.* **2015**, *20* (5), 443−450.

(8) (a) Tuteja, A.; Duxbury, P. M.; Mackay, M. E. Multifunctional Nanocomposites with Reduced Viscosity. *Macromolecules* **2007**, *40* (26), 9427−9434. (b) Malkin, A. Y.; Semakov, A. V.; Kulichikhin, V. G. Self-Organization in the Flow of Complex Fluids (Colloid and Polymer Systems): Part 1: Experimental Evidence. *Adv. Colloid Interface Sci.* **2010**, *157* (1−2), 75−90. (c) Ilyin, S. O.; Brantseva, T. V.; Gorbunova, I. Y.; Antonov, S. V.; Korolev, Y. M.; Kerber, M. L. Epoxy Reinforcement with Silicate Particles: Rheological and Adhesive Properties - Part I: Characterization of Composites with Natural and Organically Modified Montmorillonites. *Int. J. Adhes. Adhes.* **2015**, *61*, 127−136. (d) Brantseva, T.; Antonov, S.; Kostyuk, A.; Ignatenko, V.; Smirnova, N.; Korolev, Y.; Tereshin, A.; Ilyin, S. Rheological and Adhesive Properties of PIB-Based Pressure-Sensitive Adhesives with Montmorillonite-Type Nanofillers. *Eur. Polym. J.* **2016**, *76*, 228−244. (e) Yu, Q.; Yang, W.; Wang, Q.; Dong, W.; Du, M.; Ma, P. Functionalization of Cellulose Nanocrystals with γ-MPS and Its Effect on the Adhesive Behavior of Acrylic Pressure Sensitive Adhesives. *Carbohydr. Polym.* **2019**, *217*, 168−177.

(9) (a) Li, B.; Wang, X.; Bai, M.; Shen, Y. Improvement of Curing Reaction Activity of One-Component Room Temperature-Curable Epoxy Adhesive by the Addition of Functionalized Graphene Oxide. *Int. J. Adhes. Adhes.* **2020**, *98*, 102537.

(10) (a) Quaresimin, M.; Schulte, K.; Zappalorto, M.; Chandrasekaran, S. Toughening Mechanisms in Polymer Nanocomposites: From Experiments to Modelling. *Compos. Sci. Technol.* **2016**, *123*, 187−204. (b) Chen, J.-k.; Wang, G.-T.; Yu, Z.-Z.; Huang, Z.; Mai, Y.-W. Critical Particle Size for Interfacial Debonding in Polymer/Nanoparticle Composites. *Compos. Sci. Technol.* **2010**, *70* (5), 861−872. (c) Shokrieh, M. M.; Ghoreishi, S. M.; Esmkhani, M. *Toughening Mechanisms of Nanoparticle-Reinforced Polymers*; Elsevier Ltd., 2015. (d) Gholami, R.; Khoramishad, H.; da Silva, L. F. M. Glass Fiber-Reinforced Polymer Nanocomposite Adhesive Joints Reinforced with Aligned Carbon Nanofillers. *Compos. Struct.* **2020**, *253*, 112814.

(11) (a) Khanjani, J. Pressure-Sensitive Adhesive Joints. In *Adhesives and Adhesive Joints in Industry Applications*; InTechOpen, 2019; p 85667,. (b) Dahlquist, C. A. Pressure-Sensitive Adhesives. In *Treatise on Adhesion and Adhesives*; Patrick, R. L., Ed.; Marcel Dekker Ltd.: New York, 1967; p 219. (c) Tramis, O.; Brethous, R.; Hassoune-Rhabbour, B.; Fazzini, M.; Nassiet, V. Experimental Investigation on the Effect of Nanostructuration on the Adherence Properties of Epoxy Adhesives by a Probe Tack Test. *Int. J. Adhes. Adhes.* **2016**, *67*, 22−30. (d) Pandey, V.; Fleury, A.; Villey, R.; Creton, C.; Ciccotti, M. Linking Peel and Tack Performances of Pressure Sensitive Adhesives. *Soft Matter* **2020**, *16* (13), 3267−3275.

(12) (a) Antonov, S.; Brantseva, T.; Kostyuk, A.; Ignatenko, V.; Smirnova, N. Rheology and Adhesive Properties of Filled PIB-Based Pressure-Sensitive Adhesives. II. Probe Tack and 90° Peel Testing. *J. Adhes. Sci. Technol.* **2015**, *29* (24), 2635−2647. (b) Khalina, M.; Sanei, M.; Mobarakeh, H. S.; Mahdavian, A. R. Preparation of Acrylic/Silica Nanocomposites Latexes with Potential Application in Pressure Sensitive Adhesive. *Int. J. Adhes. Adhes.* **2015**, *58*, 21−27. (c) Antosik, A. K.; Mozelewska, K.; Pełech, R.; Czech, Z.; Antosik, N. A. Conductive Electric Tapes Based on Silicone Pressure-Sensitive

https://doi.org/10.1021/acsomega.1c05448
ACS Omega 2022, 7, 3844−3859

Adhesives. *Silicon* **2021**, *13* (3), 867−875. (d) Pang, B.; Ryu, C. M.; Jin, X.; Kim, H. Il. Preparation and Properties of UV Curable Acrylic PSA by Vinyl Bonded Graphene Oxide. *Appl. Surf. Sci.* **2013**, *285* (PARTB), 727−731. (e) Czech, Z.; Kowalczyk, A.; Pełech, R.; Wrobel, R.J.; Shao, L.; Bai, Y.; Swiderska, J. Świderska, J. Using of Carbon Nanotubes and Nano Carbon Black for Electrical Conductivity Adjustment of Pressure-Sensitive Adhesives. *Int. J. Adhes. Adhes.* **2012**, *36*, 20−24.

(13) Shull, K. R.; Creton, C. Deformation Behavior of Thin, Compliant Layers under Tensile Loading Conditions. *J. Polym. Sci., Part B: Polym. Phys.* **2004**, *42* (22), 4023−4043.

(14) (a) Sardeh Moghadam, R.; Moghbeli, M. R. Effect of Organoclay and Chain-Transfer Agent on Molecular Parameters and Adhesion Performance of Emulsion Pressure-Sensitive Adhesives. *J. Adhes. Sci. Technol.* **2016**, *30* (3), 284−299. (b) Zhang, M. Y.; Wang, G. H.; Yu, P.; Wang, Y. The Study of High Heat Resistance of Nano-Modified Silicone Pressure Sensitive Adhesives. *Adv. Mater. Res. Vols.* **2011**, *403*−*408*, 1106−1112.

(15) Khan, U.; May, P.; Porwal, H.; Nawaz, K.; Coleman, J. N. Improved Adhesive Strength and Toughness of Polyvinyl Acetate Glue on Addition of Small Quantities of Graphene. *ACS Appl. Mater. Interfaces* **2013**, *5* (4), 1423−1428.

(16) Tounici, A.; Martín-Martínez, J. M. Addition of Small Amounts of Graphene Oxide in the Polyol during the Synthesis of Waterborne Polyurethane Urea Adhesives for Improving Their Adhesion Properties. *Int. J. Adhes. Adhes.* **2021**, *104*, 102725.

(17) Mondal, T.; Bhowmick, A. K.; Krishnamoorti, R. Conducting Instant Adhesives by Grafting of Silane Polymer onto Expanded Graphite. *ACS Appl. Mater. Interfaces* **2014**, *6* (18), 16097−16105.

(18) Wang, L.; Shui, X.; Zheng, X.; You, J.; Li, Y. Investigations on the Morphologies and Properties of Epoxy/Acrylic Rubber/Nanoclay Nanocomposites for Adhesive Films. *Compos. Sci. Technol.* **2014**, *93*, 46−53.

(19) A. A, S.; Varghese, S.; Thomas, S. Natural Rubber Latex-Based Adhesives: Role of Nanofillers. *J. Adhes. Sci. Technol.* **2021**, *35* (4), 406−418.

(20) Moya, R.; Rodríguez-Zúñiga, A.; Vega-Baudrit, J.; Álvarez, V. Effects of Adding Nano-Clay (Montmorillonite) on Performance of Polyvinyl Acetate (PVAc) and Urea-Formaldehyde (UF) Adhesives in Carapa Guianensis, a Tropical Species. *Int. J. Adhes. Adhes.* **2015**, *59*, 62−70.

(21) Ghosh, P. K.; Kumar, K.; Preeti, P.; Rajoria, M.; Misra, N. Superior Dissimilar Adhesive Joint of Mild Steel and Aluminium Using UDM Processed Epoxy Based TiO2 Nano-Filler Composite Adhesive. *Compos. Part B Eng.* **2016**, *99* (1554), 224−234.

(22) Maghsoudian, S.; Salimi, A.; Mirzataheri, M. The Effect of Nanoalumina Silanisation in Tetraglycidylether Epoxy Adhesive. *Int. J. Adhes. Adhes.* **2019**, *92* (March), 119−124.

(23) Heo, J. H.; Lee, J. W.; Lee, B.; Cho, H. H.; Lim, B.; Lee, J. H. Chemical Effects of Organo-Silanized SiO2 Nanofillers on Epoxy Adhesives. *J. Ind. Eng. Chem.* **2017**, *54*, 184−189.

(24) Basak, G. C.; Kumar, K. D.; Bandyopadhyay, A.; Bhowmick, A. K. Elegant Way of Strengthening Polymer-Polymer Interface Using Nanoclay. *ACS Appl. Mater. Interfaces* **2010**, *2* (10), 2933−2943.

(25) Kumar, K. D.; Tsou, A. H.; Bhowmick, A. K. Unique Tackification Behavior of Needle-like Sepiolite Nanoclay in Brominated Isobutylene-Co-p-Methylstyrene (BIMS) Rubber. *Macromolecules* **2010**, *43* (9), 4184−4193.

https://doi.org/10.1021/acsomega.1c05448
ACS Omega 2022, 7, 3844−3859